

VU Research Portal

Relating a reified adaptive network's structure to its emerging behaviour for bonding by homophily

Treur, Jan

published in

Network-Oriented Modeling for Adaptive Networks: Designing Higher-Order Adaptive Biological, Mental and Social Network Models

2020

DOI (link to publisher)

[10.1007/978-3-030-31445-3_13](https://doi.org/10.1007/978-3-030-31445-3_13)

document version

Publisher's PDF, also known as Version of record

document license

Article 25fa Dutch Copyright Act

[Link to publication in VU Research Portal](#)

citation for published version (APA)

Treur, J. (2020). Relating a reified adaptive network's structure to its emerging behaviour for bonding by homophily. In J. Treur (Ed.), *Network-Oriented Modeling for Adaptive Networks: Designing Higher-Order Adaptive Biological, Mental and Social Network Models* (pp. 321-352). (Studies in Systems, Decision and Control; Vol. 251). Springer International Publishing AG. https://doi.org/10.1007/978-3-030-31445-3_13

General rights

Copyright and moral rights for the publications made accessible in the public portal are retained by the authors and/or other copyright owners and it is a condition of accessing publications that users recognise and abide by the legal requirements associated with these rights.

- Users may download and print one copy of any publication from the public portal for the purpose of private study or research.
- You may not further distribute the material or use it for any profit-making activity or commercial gain
- You may freely distribute the URL identifying the publication in the public portal ?

Take down policy

If you believe that this document breaches copyright please contact us providing details, and we will remove access to the work immediately and investigate your claim.

E-mail address:

vuresearchportal.ub@vu.nl

Chapter 13

Relating a Reified Adaptive Network's Structure to Its Emerging Behaviour for Bonding by Homophily



Abstract In this chapter it is analysed how emerging behaviour in an adaptive social network for bonding can be related to characteristics of the adaptive network's structure, which includes the structure of the adaptation principles incorporated. In particular, this is addressed for adaptive social networks for bonding based on homophily and for community formation in such adaptive social networks. To this end, relevant characteristics of the reified network structure (including the adaptation principle) have been identified, such as a tipping point for similarity as used for homophily. Applying network reification, the adaptive network characteristics are represented by reification states in the extended network, and adaptation principles are described by characteristics of these reification states, in particular their connectivity characteristics (their connections) and their aggregation characteristics (in terms of their combination functions). According to this network reification approach, as one of the results it has been found how the emergence of communities strongly depends on the value of this similarity tipping point. Moreover, it is shown that some characteristics entail that the connection weights all converge to 0 (for persons in different communities) or 1 (for persons within one community).

13.1 Introduction

In this chapter, the emerging behaviour of the coevolution of social contagion (Levy and Nail 1993) and bonding by homophily (McPherson et al. 2001; Pearson et al. 2006) is analysed. In particular, it is analysed how emerging communities based on the coevolution of social contagion and bonding by homophily can be related to characteristics of the adaptive network's structure. For this adaptive case, this network structure includes the structure of the homophily adaptation principle that is incorporated. The homophily adaptation principle expresses how 'being alike' strengthens the connection between two persons (McPherson et al. 2001; Pearson et al. 2006). Social contagion implies that the stronger two persons are connected, the more they will become alike (Levy and Nail 1993). Thus a reciprocal

causal relation between the two processes occurs. It is known from simulations (Axelrod 1997; Holme, and Newman 2006; Sharpanskykh and Treur 2014; Vazquez 2013; Vazquez et al. 2007) that the emerging behaviour of adaptive network models combining these two processes as a form of coevolution often shows community formation. In the resulting network structure within a community persons have high mutual connection weights and a high extent of 'being alike', and persons from different communities have low mutual connection weights and a low extent of 'being alike'.

Relevant characteristics of the network and the homophily adaptation principle have been identified, such as a tipping point for homophily. As one of the results, it has been found how the emergence of communities strongly depends on the value of this tipping point. Moreover, it is shown that some characteristics of the reified network structure entail that the connection weights all converge to 0 (for states in different emerging communities) or 1 (for states within one emerging community).

In general, it is a challenging issue for dynamic models to predict what patterns of behaviour will emerge, and how their emergence depends on the structure of the model. The latter includes chosen values used for characteristics of the model's structure (and settings). This also applies to network models, where behaviour depends in some way on the network structure, defined by network characteristics such as connectivity (connections and their weights); e.g., Turnbull et al. (2018). In this context, the issue is how emerging network behaviour relates to network structure; for example, see (Treur 2018a). It can be an even more challenging issue when coevolution that occurs in adaptive networks is considered, in which case by a mutual causal interaction both the states and the network characteristics change over time. In this case the connections in the network change according to certain adaptation principles which depend on certain adaptation characteristics.

In the current chapter, the emergence of communities based on the coevolution of social contagion (Levy and Nail 1993) and bonding by homophily (McPherson et al. 2001; Pearson et al. 2006) is analysed in some depth. By mathematical analysis, it is found out how emerging communities relate to the characteristics of the network and of the specific homophily adaptation principle used in combination with a social contagion principle.

The issue was addressed using the Network-Oriented Modeling approach based on temporal-causal networks (Treur 2016, 2019) as a vehicle. For temporal-causal networks, characteristics of the network structure are Connectivity, Aggregation, and Timing, represented by connection weights, combination functions, and speed factors, respectively. For the type of adaptive networks considered, the connection weights are dynamic based on the homophily principle. When network reification, see Chap. 3 or (Treur 2018d) is applied, these adaptation principles are represented as an extended part of the network using certain reification states in the network extension. These reification states have their own (reified) network structure characteristics defining their Connectivity, Aggregation, and Timing by their connection weights, speed factors and combination functions. So, the challenge then is how the emergent behaviour of the reified adaptive network depends on these characteristics and, in particular, on Aggregation characteristics of reification states

in terms of properties of the combination functions used by them for bonding by homophily.

In Fig. 13.1 the basic relation between structure and dynamics of a reified network model is indicated by the horizontal arrow in the lower part representing the base level. For a reified network these also apply to the reification states. The network structure characteristics (addressed in Sect. 13.5) cover properties of the adaptation principle based on bonding by homophily represented by the reification states at the reification level (in Sect. 13.5.1) and properties of the social contagion in the base network (in Sect. 13.5.2). Properties of the behaviour are discussed in Sect. 13.4 first by a number of simulation experiments, and they are formalised and related to the network structure properties (the horizontal arrow in the upper part of Fig. 13.1) in Sect. 13.6.

In the research reported here characteristics of the combination function describing the aggregation used by the homophily adaptation principle have been identified that play an important role in community formation, among which the tipping point for the similarity between two persons. This is the point where ‘being alike’ turns into ‘not being alike’, or conversely. In this chapter, results are discussed that have been proven mathematically for this relationship between network structure and network behavior for the coevolution process. In particular, for emerging communities what the connections become between persons from one community or persons from different communities, and how different persons from one community or from different communities become. Note that these results have not been proven for one specific model or combination function, but for whole classes of models with a variety of combination functions that fulfill certain properties.

In this chapter, in Sect. 13.2 the Network-Oriented Modeling approach used is briefly outlined. In Sect. 13.3 adaptive networks based on homophily are described and a number of functions that can be used to model them. Section 13.4 shows some example simulations. In Sect. 13.5 relevant reified network structure characteristics are defined that are used in Sect. 13.6 to prove results on the relation between network structure and behaviour. In Sect. 13.7 it is shown how the obtained results relate to the strongly connected components of a network. In Sect. 13.8 an overview is presented of various simulation experiments concerning bonding by homophily, most of which in relation to empirical data. Finally, Sect. 13.9 is a discussion.

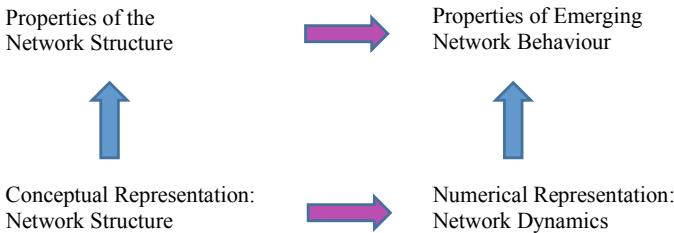


Fig. 13.1 Bottom layer: the conceptual representation of a reified network model defines the numerical representation. Top layer: properties of reified network structure entail properties of emerging reified network behaviour

13.2 Network-Oriented Modeling by Temporal-Causal Networks

In order to undertake any mathematical analysis of networks, in the first place, a solid definition of the concept of network is needed, based on well-defined semantics. In the current chapter, the interpretation of connections based on causality and dynamics forms a basis of the structure and semantics of the considered networks. It is a deterministic dynamic modeling approach, for example in the line of (Ashby 1960), in contrast to, stochastic modeling approaches as, for example, used in Axelrod (1997). It can be positioned as a branch in the causal modelling area which has a long tradition in AI; e.g., see Kuipers and Kassirer (1983), Kuipers (1984), Pearl (2000). It distinguishes itself by a dynamic perspective on causal relations, according to which causal relations exert causal effects over time, and these causal relations themselves can also change over time.

More specifically, the nodes in a network are interpreted here as states (or state variables) that vary over time, and the connections are interpreted as causal relations that define how each state can affect other states over time. This type of network has been called a *temporal-causal network* (Treur 2016b); note that the word temporal here refers to the causality, not to the network. Temporal-causal networks that themselves change over time as well are called adaptive temporal-causal networks; e.g., Gross and Sayama (2009). So, in cases of adaptive temporal-causal networks, in addition to the node states also the connections are assumed to change over time and are therefore treated like states as well.

A conceptual representation of a temporal-causal network model by a *labeled graph* provides a fundamental basis. Such a conceptual representation includes representing in a declarative manner states (also called nodes) and connections between them that represent (causal) impacts of states on each other. This part of a conceptual representation is often depicted in a *conceptual picture* by a graph with nodes and directed connections. However, a *complete conceptual representation* of a temporal-causal network model also includes a number of labels for such a graph. A notion of *strength of a connection* is used as a label for connections, some way to *aggregate multiple causal impacts* on a state is used, and a notion of *speed of change* of a state is used for timing of the processes. Note that states have one value; they can relate one by one to states of persons or agents, for example, the strength of their opinion states. It is also possible to model each person by more than one state, for example, an opinion and an emotion state per person. In such a case a person does not relate to a single state but to a subnetwork consisting of multiple states.

The three described notions for network structure characteristics Connectivity, Aggregation, and Timing, are called connection weight $\omega_{X,Y}$, combination function $c_Y(\dots)$, and speed factor η_Y . They make the graph of states and connections a labeled graph (e.g., see Fig. 13.2), and form the defining structure of a temporal-causal network model in the form of a conceptual representation; for a summary, see also Table 13.1, top half: rows 1–5. Note that although in general that is not always required, for the current chapter all connection weights are assumed nonnegative: $\omega_{X,Y} \in [0, 1]$ for all X and Y .

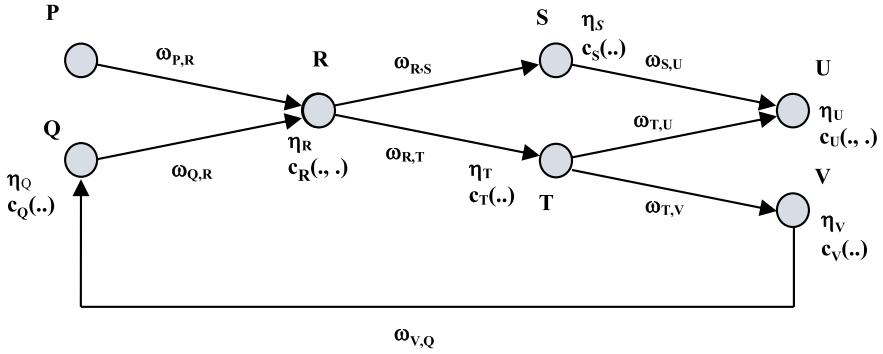


Fig. 13.2 Conceptual representation of an example temporal-causal network model: adopted from Treur (2016b)

The interpretation of a network based on causality and dynamics can be expressed in a formal-numerical way, thus associating semantics to any conceptual temporal-causal network representation in a detailed numerical-mathematically defined manner. For a summary, see Table 13.1, bottom half: rows 6 to 10. This shows how a conceptual representation based on states and connections enriched with labels for connection weights, combination functions, and speed factors, can be transformed into a numerical representation (Treur 2016b, Chap. 2). A more detailed explanation of the difference equation format, taken from Treur (2016b, Chap. 2, pp. 60–61), is as follows; see also Fig. 13.3. The aggregated impact value $\text{aggimpact}_Y(t)$ at time t pushes the value of Y up or down, depending on how it compares to the current value of Y . So, $\text{aggimpact}_Y(t)$ is compared to the current value $Y(t)$ of Y at t by taking the difference between them (also see Fig. 13.3): $\text{aggimpact}_Y(t) - Y(t)$. If this difference is positive, which means that $\text{aggimpact}_Y(t)$ at time t is higher than the current value of Y at t , in the time step from t to $t + \Delta t$ (for some small Δt) the value $Y(t)$ will increase in the direction of the higher value $\text{aggimpact}_Y(t)$. This increase is done proportional to the difference, with proportion factor $\eta_Y \Delta t$: the increase is $\eta_Y [\text{aggimpact}_Y(t) - Y(t)] \Delta t$; see Fig. 13.3. By this format, the parameter η_Y indeed acts as a speed factor by which it can be specified how fast state Y should change upon causal impact.

There are many different approaches possible to address the issue of combining multiple causal impacts. To provide sufficient flexibility, the Network-Oriented Modelling approach based on temporal-causal networks incorporates for each state a way to specify how multiple causal impacts on this state are aggregated by a combination function. For this aggregation, a library with a number of standard combination functions are available as options (currently 35), but also own-defined functions can be added. The difference equations in Fig. 13.3 and in the last row in Table 13.1 constitute the overall numerical representation of the temporal-causal network model and can be used for simulation and mathematical analysis; it can also be written in differential equation format:

Table 13.1 Conceptual and numerical representations of a temporal-causal network model

Concept	Conceptual representation	Explanation
States and connections	$X, Y, X \rightarrow Y$	Describes the nodes and links of a network structure (e.g., in graphical or matrix format)
Connection weight	$\omega_{X,Y}$	The <i>connection weight</i> $\omega_{X,Y} \in [-1, 1]$ represents the strength of the causal impact of state X on state Y through connection $X \rightarrow Y$
Aggregating multiple impacts on a state	$\mathbf{c}_Y(\cdot)$	For each state Y (a reference to) a <i>combination function</i> $\mathbf{c}_Y(\cdot)$ is chosen to combine the causal impacts of other states on state Y
Timing of the effect of causal impact	η_Y	For each state Y a <i>speed factor</i> $\eta_Y \geq 0$ is used to represent how fast a state is changing upon causal impact

Concept	Numerical representation	Explanation
State values over time t	$Y(t)$	At each time point t each state Y in the model has a real number value, usually in $[0, 1]$
Single causal impact	$\mathbf{impact}_{X,Y}(t)$ $= \omega_{X,Y} X(t)$	At t state X with a connection to state Y has an impact on Y , using connection weight $\omega_{X,Y}$
Aggregating multiple causal impacts	$\mathbf{aggimpact}_Y(t)$ $= \mathbf{c}_Y(\mathbf{impact}_{X_1,Y}(t), \dots, \mathbf{impact}_{X_k,Y}(t))$ $= \mathbf{c}_Y(\omega_{X_1,Y}X_1(t), \dots, \omega_{X_k,Y}X_k(t))$	The aggregated causal impact of multiple states X_i on Y at t , is determined using combination function $\mathbf{c}_Y(\cdot)$
Timing of the causal effect	$Y(t + \Delta t) = Y(t) + \eta_Y[\mathbf{aggimpact}_Y(t) - Y(t)]\Delta t$ $= Y(t) + \eta_Y[\mathbf{c}_Y(\omega_{X_1,Y}X_1(t), \dots, \omega_{X_k,Y}X_k(t)) - Y(t)]\Delta t$	The causal impact on Y is exerted over time gradually, using speed factor η_Y ; here the X_i are all states with outgoing connections to state Y

$$Y(t + \Delta t) = Y(t) + \eta_Y[\mathbf{c}_Y(\omega_{X_1,Y}X_1(t), \dots, \omega_{X_k,Y}X_k(t)) - Y(t)]\Delta t \quad (13.1)$$

$$\mathbf{d}Y(t)/\mathbf{d}t = \eta_Y[\mathbf{c}_Y(\omega_{X_1,Y}X_1(t), \dots, \omega_{X_k,Y}X_k(t)) - Y(t)]$$

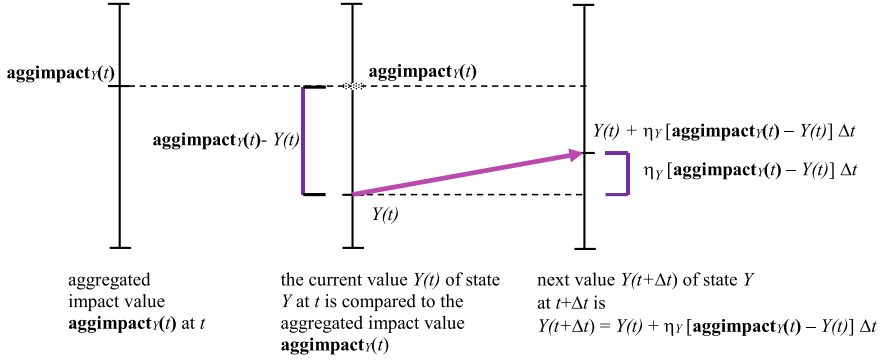


Fig. 13.3 How $\text{aggimpact}_Y(t)$ makes a difference for state $Y(t)$ in the time step from t to $t + \Delta t$

For reified adaptive networks, connection weights are dynamic and therefore handled by reification states for them, with their own connectivity and aggregation characteristics in terms of connections and combination functions. This will be shown in more detail in Sects. 13.3–13.5.

Often used examples of combination functions are the *identity* function $\text{id}(\cdot)$ for states with impact from only one other state, the *scaled sum* function $\text{ssum}_\lambda(\cdot)$ with scaling factor λ , and the *advanced logistic sum* combination function $\text{alogistic}_{\sigma,\tau}(\cdot)$ with steepness σ and threshold τ :

$$\begin{aligned} \text{id}(V) &= V \\ \text{ssum}_\lambda(V_1, \dots, V_k) &= \frac{V_1 + \dots + V_k}{\lambda} \\ \text{alogistic}_{\sigma,\tau}(V_1, \dots, V_k) &= \left[\frac{1}{1 + e^{-\sigma(V_1 + \dots + V_k - \tau)}} - \frac{1}{1 + e^{\sigma\tau}} \right] (1 + e^{-\sigma\tau}) \end{aligned} \quad (13.2)$$

Note that for $\lambda = 1$, the scaled sum function is just the sum function $\text{sum}(\cdot)$, and this sum function can also be used as the identity function in case of one incoming connection. In addition to the above functions, a *Euclidean combination function* is defined as

$$\mathbf{c}(V_1, \dots, V_k) = \mathbf{eucl}_{n,\lambda}(V_1, \dots, V_k) = \sqrt[n]{\frac{V_1^n + \dots + V_k^n}{\lambda}} \quad (13.3)$$

where n is the *order* (which can be any positive natural number but also any positive real number), and λ is a scaling factor. This can be used when all connection weights are non-negative, but in the specific case that n is an odd natural number, also negative connection weights can be allowed. A Euclidean combination function is called *normalised* if the scaling factor λ is chosen in such a way that $\mathbf{c}(\omega_{X_1,Y}, \dots, \omega_{X_k,Y}) = 1$; this is achieved for $\lambda = \omega_{X_1,Y}^n + \dots + \omega_{X_k,Y}^n$. Note that for $n = 1$ (first order) the scaled sum function is obtained:

$$\mathbf{eucl}_{1,\lambda}(V_1, \dots, V_k) = \mathbf{ssum}_\lambda(V_1, \dots, V_k) \quad (13.4)$$

Then $\lambda = \omega_{X_1,Y} + \dots + \omega_{X_k,Y}$ makes it normalised. For $n = 2$ it is the second-order Euclidean combination function $\mathbf{eucl}_{2,\lambda}(\cdot)$ defined by:

$$\mathbf{eucl}_{2,\lambda}(V_1, \dots, V_k) = \sqrt{\frac{V_1^2 + \dots + V_k^2}{\lambda}} \quad (13.5)$$

Such a second-order Euclidean combination function is also often applied in aggregating the error value in optimisation and in parameter tuning using the root-mean-square deviation (RMSD), based on the Sum of Squared Residuals (SSR).

13.3 Reified Adaptive Networks for Bonding Based on Homophily

The homophily principle addresses bonding between persons. It describes how connections between two persons are strengthened or weakened depending on the extent of similarity between them: more ‘being alike’ will make the persons more ‘like each other’ (McPherson et al. 2001; Pearson et al. 2006). This is modelled by how the states $X(t)$ and $Y(t)$ the persons X and Y have at time t compare to each other, for example, indicating whether at time t they enjoy being physically active (high value) or not (low value), or indicating the extent to which they agree with a certain opinion. According to the homophily principle the weight $\omega_{X,Y}$ of the connection from X to Y is changing over time dynamically, depending on how the state levels $X(t)$ and $Y(t)$ differ.

13.3.1 Modeling the Bonding by Homophily Adaptation Principle by Reification

As the connection weight $\omega_{X,Y}$ is dynamic, using network reification it is handled as a reification state $\mathbf{W}_{X,Y}$ with its own combination function $\mathbf{c}_{\mathbf{W}_{X,Y}}(V_1, V_2, W)$, called in this chapter a *homophily combination function*. Here V_1 and V_2 refer to the values for $X(t)$ and $Y(t)$ of the states X and Y involved and W to the value $\mathbf{W}_{X,Y}(t)$ of the reified connection weight $\mathbf{W}_{X,Y}$. See Fig. 13.4, where the homophily functions $\mathbf{c}_{\mathbf{W}_{X_1,Y}}(V_1, V_2, W)$ and $\mathbf{c}_{\mathbf{W}_{X_2,Y}}(V_1, V_2, W)$ are indicated as labels (like the labels in Fig. 13.2) for the reification states $\mathbf{W}_{X_1,Y}$ and $\mathbf{W}_{X_2,Y}$. Similarly labels for adaptation speed can be added, and labels for the incoming connections for the reification states.

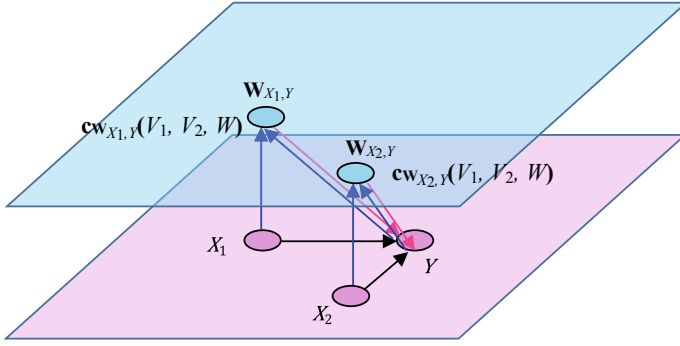


Fig. 13.4 Homophily combination functions as labels in the reified network

Then the standard difference and differential equation format for temporal-causal networks as shown in Sect. 13.2 is applied:

$$\begin{aligned} \mathbf{W}_{X,Y}(t + \Delta t) &= \mathbf{W}_{X,Y}(t) + \eta_{\mathbf{W}_{X,Y}} [\mathbf{cw}_{X,Y}(X(t), Y(t), \mathbf{W}_{X,Y}(t)) - \mathbf{W}_{X,Y}(t)] \Delta t \\ d\mathbf{W}_{X,Y}/dt &= \eta_{\mathbf{W}_{X,Y}} [\mathbf{cw}_{X,Y}(X, Y, \mathbf{W}_{X,Y}) - \mathbf{W}_{X,Y}] \end{aligned} \quad (13.6)$$

Here $\eta_{\mathbf{W}_{X,Y}}$ is the speed factor of connection weight reification state $\mathbf{W}_{X,Y}$. It determines how fast adaptation takes place. Note that

- $\mathbf{W}_{X,Y}(t)$ increases at t if and only if $\mathbf{cw}_{X,Y}(X(t), Y(t), \mathbf{W}_{X,Y}(t)) > \mathbf{W}_{X,Y}(t)$
- $\mathbf{W}_{X,Y}(t)$ decreases if and only if $\mathbf{cw}_{X,Y}(X(t), Y(t), \mathbf{W}_{X,Y}(t)) < \mathbf{W}_{X,Y}(t)$
- $\mathbf{W}_{X,Y}(t)$ is stationary if and only if $\mathbf{cw}_{X,Y}(X(t), Y(t), \mathbf{W}_{X,Y}(t)) = \mathbf{W}_{X,Y}(t)$

Specific adaptation principles formalising bonding by homophily can be obtained by picking specific functions for the homophily combination function $\mathbf{cw}_{X,Y}(V_1, V_2, W)$ for a given application domain, or even different combination functions $\mathbf{cw}_{X,Y}(V_1, V_2, W)$ for different persons within a given domain. There are many options for such choices; see, for example, Table 13.2 and Fig. 13.5. Therefore it may be more useful to define classes of such homophily combination functions characterised by certain properties of them. Then as will be shown in Sect. 13.6, results can be proven for such a class instead of for each homophily combination function separately. Formal definitions of such properties of the function $\mathbf{cw}_{X,Y}(V_1, V_2, W)$ will be given in Sect. 13.5, but here some examples of homophily combination functions are shown.

13.3.2 Various Examples of Homophily Combination Functions

A very simple example of a homophily combination function $\mathbf{cw}_{X,Y}(V_1, V_2, W)$ is a linear function in $D = |V_1 - V_2|$ defined as follows:

Table 13.2 Different options for combination functions $\mathbf{cw}_{\omega_{X,Y}}(V_1, V_2, W)$ for the homophily principle based on a tipping point τ ; for the graphs depending on $D = |V_1 - V_2|$, see Fig. 13.5

Function type	Function name	Numerical representation	Parameters in Fig. 13.5
Simple Linear	$\mathbf{slhomo}_{\tau,\alpha}(V_1, V_2, W)$	$W + \alpha W (1 - W) (\tau - D)$	$\alpha = 6$
Simple quadratic 1	$\mathbf{sq1homo}_{\tau,\alpha}(V_1, V_2, W)$	$W + \alpha W (1 - W) (\tau^2 - D^2)$	$\alpha = 6$
Simple quadratic 2	$\mathbf{sq2homo}_{\tau,\alpha,\delta}(V_1, V_2, W)$	$W + \alpha ((\tau + \delta)^2 - (D + \delta)^2)$	$\delta = 0.15, \alpha = 10$
Cubic	$\mathbf{cubehomo}_{\tau,\alpha}(V_1, V_2, W)$	$W + \alpha (1 - W) (1 - D/\tau)^3$	$\alpha = 0.9$
Logistic 1	$\mathbf{log1homo}_{\tau,\sigma}(V_1, V_2, W)$	$\frac{W}{W + (1 - W)e^{(D - \tau)}}$	$\sigma = 10$
Logistic 2	$\mathbf{slog2homo}_{\tau,\sigma,\alpha}(V_1, V_2, W)$	$W + \alpha \frac{W(1 - W)}{1 + e^{-(D - \tau)}}$	$\sigma = 4, \alpha = 5$
Sine-based	$\mathbf{sinhomo}_{\tau,\alpha}(V_1, V_2, W)$	$W - \alpha (1 - W) \sin(\pi (D - \tau)/2)$	$\alpha = 2$
Tangent-based	$\mathbf{tanhomo}_{\tau,\alpha}(V_1, V_2, W)$	$W - \alpha (1 - W) \tan(\pi (D - \tau)/2)$	$\alpha = 2$
Exponential	$\mathbf{exphomo}_{\tau,\sigma}(V_1, V_2, W)$	$1 - (1 - W) e^{\sigma(D - \tau)}$	$\sigma = 10$

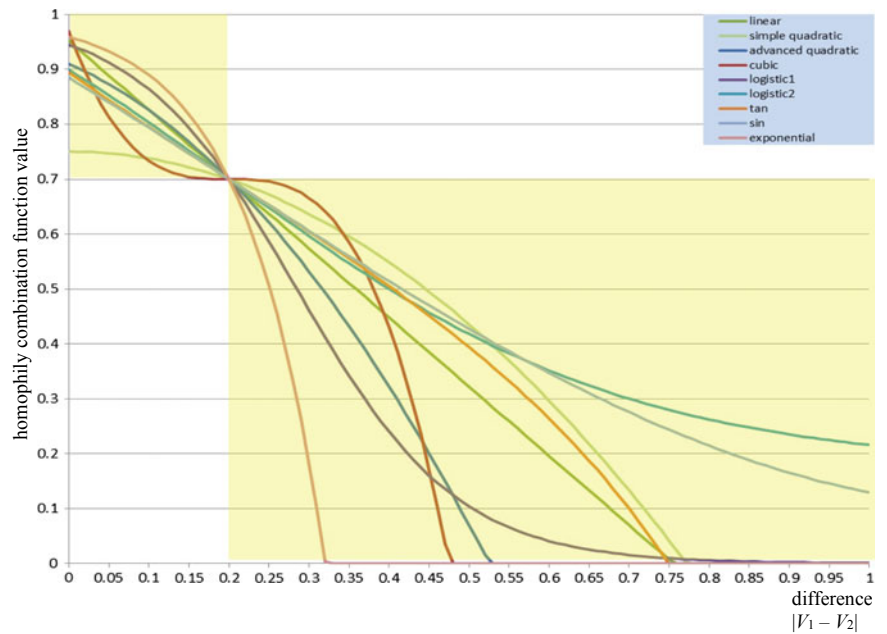


Fig. 13.5 Graphs for different options for homophily combination functions $\mathbf{cw}_{\omega_{X,Y}}(V_1, V_2, W)$ with tipping point $\tau = 0.2$ and $W = 0.7$ with difference $D = |V_1 - V_2|$ on the horizontal axis

$$\mathbf{c}_{W_{X,Y}}(V_1, V_2, W) = W + \beta(\tau - D) \quad (13.7)$$

Here β is a modulation factor that still can be chosen, and τ is a tipping point (or threshold) parameter. This function may have the disadvantage that when $W = 0$ it may be negative (when $D > \tau$) or when $W = 1$ it may be higher than 1 (when $D < \tau$), so that it has to be cut off to avoid that the reified connection weight value $\mathbf{W}_{X,Y}$ goes outside the interval $[0, 1]$. This can also be remedied in a smooth manner by choosing β as a function $\beta(W) = \alpha W(1 - W)$ of W which can suppress the term $\tau - D$ when W comes closer to 0 or 1. This function makes that $\mathbf{W}_{X,Y}$ will not cross the boundaries 0 and 1:

$$\mathbf{c}_{W_{X,Y}}(V_1, V_2, W) = W + \alpha W(1 - W)(\tau - |V_1 - V_2|) \quad (13.8)$$

Here α is a modulation or amplification parameter; the higher its value, the stronger the effect (either positive or negative) of homophily on the connection. Using this homophily combination function, the dynamic relations for $\mathbf{W}_{X,Y}$ are:

$$\begin{aligned} d\mathbf{W}_{X,Y}/dt &= \eta_{W_{X,Y}} \alpha \mathbf{W}_{X,Y} (1 - \mathbf{W}_{X,Y}) (\tau - |X - Y|) \\ \mathbf{W}_{X,Y}(t + \Delta t) &= \mathbf{W}_{X,Y}(t) + \eta_{W_{X,Y}} \alpha \mathbf{W}_{X,Y}(t) (1 - \mathbf{W}_{X,Y}(t)) (\tau - |X(t) - Y(t)|) \Delta t \end{aligned} \quad (13.9)$$

As a variant of this homophily combination function $\mathbf{c}_{W_{X,Y}}(V_1, V_2, W)$ that is linear in D , the following function can be obtained as a quadratic function of $D = |V_1 - V_2|$:

$$\mathbf{c}_{W_{X,Y}}(V_1, V_2, W) = W + \alpha W(1 - W)(\tau^2 - (V_1 - V_2)^2) \quad (13.10)$$

Using this combination function, the dynamic relations for the reification state $\mathbf{W}_{X,Y}$ are:

$$\begin{aligned} d\mathbf{W}_{X,Y}/dt &= \eta_{W_{X,Y}} \alpha \mathbf{W}_{X,Y} (1 - \mathbf{W}_{X,Y}) (\tau - (X - Y)^2) \\ \mathbf{W}_{X,Y}(t + \Delta t) &= \mathbf{W}_{X,Y}(t) + \eta_{W_{X,Y}} \alpha \mathbf{W}_{X,Y}(t) (1 - \mathbf{W}_{X,Y}(t)) (\tau - (X(t) - Y(t))^2) \Delta t \end{aligned} \quad (13.11)$$

In Table 13.2 and Fig. 13.5 these linear and quadratic combination function and a number of other examples of homophily combination functions are depicted, with $D = |V_1 - V_2|$ on the horizontal axis and $\mathbf{c}_{W_{X,Y}}(V_1, V_2, W)$ on the vertical axis for $\tau = 0.2$ and $W = 0.7$. In Sect. 13.6 the results that have been proven are general in the sense that they apply to all of such functions, not just one specific function. To this end, in Sect. 13.5 relevant properties shared by these functions are defined. The simple linear combination function $\mathbf{slhomo}_{\tau,\alpha}(V_1, V_2, W)$ was used in Blankendaal et al. (2016), and the simple quadratic combination function $\mathbf{sqhom}_{\tau,\alpha}(V_1, V_2, W)$ in

van Beukel et al. (2017). A more advanced logistic combination function based on $\text{log2homo}_{\tau,\sigma,\alpha}(V_1, V_2, W)$ was explored in Boomgaard et al. (2018).

13.4 Example Simulations for the Coevolution of Social Contagion and Bonding

In this section, a few example simulations for the coevolution of social contagion and bonding based on homophily are described. It will be shown how communities emerge and more specifically how their emergence depends on properties of the chosen functions for homophily. These examples will be used in Sect. 13.6 to illustrate the results that have been proven. The examples concern a fully connected social network of 10 states with speed factors $\eta_Y = 0.1$ for states Y and initial values $\mathbf{W}_{X,Y}(0)$ for the reified connection weight from state X to state Y as shown in Table 13.3.

As combination functions for social contagion for the states, the normalised scaled sum functions were used, and as combination functions for the connections for each $\mathbf{W}_{X,Y}$ the simple linear homophily function $\text{slhomo}_{\tau,\alpha}(V_1, V_2, W)$ with tipping point $\tau = 0.1$, and speed factor $\eta_{\mathbf{W}_{X,Y}} = 0.4$. The graphs in the left-hand side of Figs. 13.6 and 13.7 show time on the horizontal axis and activation values of states at the vertical axis until it ends up in an equilibrium state, i.e., all values become constant. In the same figures on the right-hand side matrices with the final connection weights are shown.

13.4.1 Simulations for Varying Homophily Modulation Factor

The homophily modulation factor α is varying from 1 to 10 in Fig. 13.6, and from 11 to 15 in Fig. 13.7. More specifically, at the left-hand side of Figs. 13.6 and 13.7 graphs of simulations of the state values are shown up to time point 100

Table 13.3 Connection matrix for the initial connection weights and state speed factor for the example network

Connections	X_1	X_2	X_3	X_4	X_5	X_6	X_7	X_8	X_9	X_{10}
X_1		0.1	0.2	0.1	0.2	0.15	0.1	0.25	0.25	0.1
X_2	0.25		0.25	0.2	0.1	0.2	0.15	0.25	0.25	0.25
X_3	0.1	0.25		0.1	0.2	0.15	0.1	0.25	0.1	0.15
X_4	0.25	0.15	0.25		0.15	0.8	0.25	0.15	0.25	0.25
X_5	0.25	0.2	0.1	0.2		0.25	0.2	0.1	0.2	0.15
X_6	0.25	0.1	0.25	0.25	0.25		0.1	0.25	0.25	0.1
X_7	0.2	0.1	0.2	0.15	0.2	0.2		0.2	0.15	0.25
X_8	0.1	0.25	0.1	0.25	0.05	0.15	0.25		0.1	0.25
X_9	0.25	0.15	0.25	0.15	0.2	0.1	0.2	0.15		0.15
X_{10}	0.2	0.25	0.2	0.2	0.1	0.2	0.15	0.8	0.2	

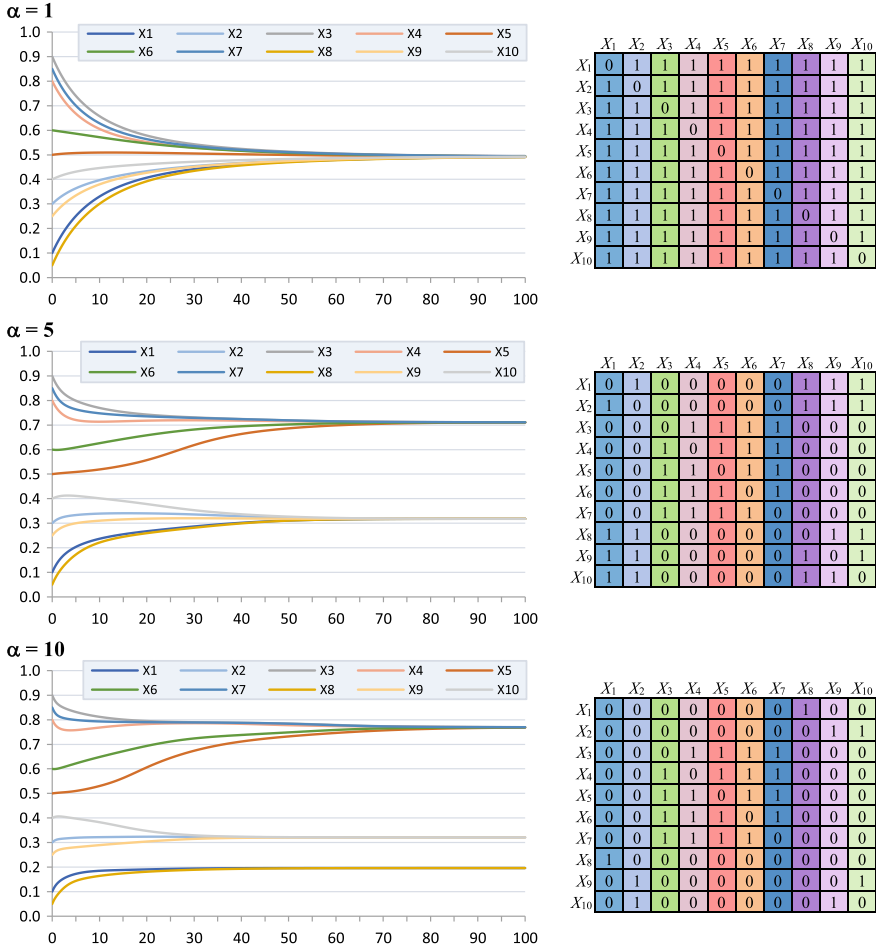


Fig. 13.6 Simulations of the example network for homophily modulation factor $\alpha = 1, 5$ and 10

(with $\Delta t = 0.05$); at the right-hand side the connection matrices are shown at time point 500 (with $\Delta t = 0.25$), with an accuracy of 3 digits (0 means < 0.001 , 1 means > 0.999). It turns out that all connection weights converge to 0 or 1.

Note that the modulation factor α models the strength of the effect of homophily. A higher α makes that connections change earlier in the coevolution process (compared to the pace of the social contagion) and due to that more clusters occur, as can be seen in Fig. 13.6. For $\alpha = 1$ all states end up in one cluster (all become connected by weights 1), for $\alpha = 5$ in two clusters (two subgroups of states $\{X_1, X_2, X_8, X_9, X_{10}\}$ and $\{X_3, X_4, X_5, X_6, X_7\}$ get connections with weight 1 and form clusters in this way; between these clusters the weights are 0), and for $\alpha = 10$ in three clusters: $\{X_1, X_8\}$, $\{X_2, X_9, X_{10}\}$ and $\{X_3, X_4, X_5, X_6, X_7\}$). Moreover, it can be observed that no clusters emerge with state values at a distance less than tipping point $\tau = 0.1$.

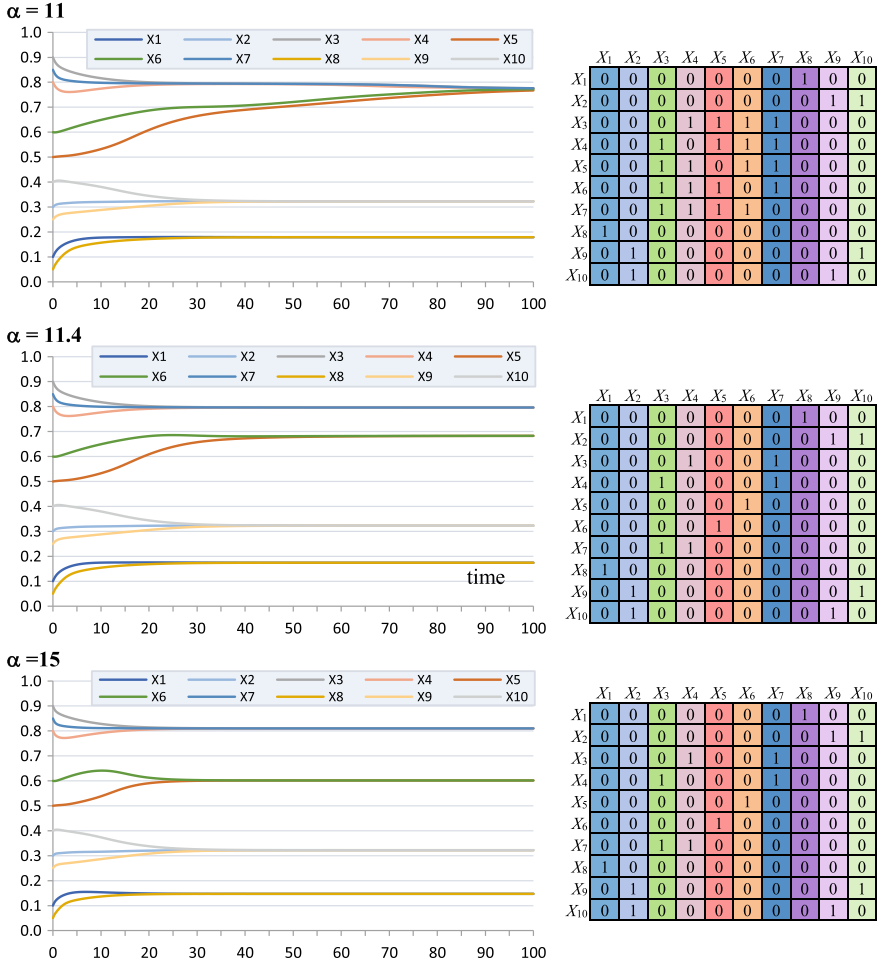


Fig. 13.7 Simulations of the example network for homophily modulation factor $\alpha = 11, 11.4$ and 15

13.4.2 Exploring the Birth of an Extra Cluster

Still increasing the modulation factor α , Fig. 13.7 zooms in at the birth of a fourth cluster. For $\alpha = 11$ it can be seen that for the cluster $\{X_3, X_4, X_5, X_6, X_7\}$ the states X_5 and X_6 join X_3, X_4 , and X_7 in a very late stage, and (compared to the case $\alpha = 10$ in Fig. 13.6) even a slight hesitation for that may be observed from time point 20 to 40 while the values of X_5 and X_6 (around 0.7) have distance of about the tipping point $\tau = 0.1$ from the values (around 0.8) for X_3, X_4 , and X_7 . This hesitation can be confirmed, as increasing the modulation factor α by just 0.4 to 11.4 shows how a fourth separate cluster emerges for $\{X_5, X_6\}$. This fourth cluster converges to state

value 0.683 whereas the other cluster $\{X_3, X_4, X_7\}$ converges to state value 0.796, which is a difference of 0.113: just above the tipping point $\tau = 0.1$. This may suggest that the model keeps the clusters at a distance of at least τ ; this is one of the issues that will be analysed further in Sect. 13.6. For higher values of α , such as $\alpha = 15$ no more than these four clusters emerge.

13.5 Relevant Aggregation Characteristics for Bonding by Homophily and for Social Contagion

This section addresses definitions for the characteristics for the network structure and in particular also for the homophily adaptation principle that have been identified as relevant for the adaptive network's behavior (following the upward arrow in the left side of Fig. 13.1).

13.5.1 Relevant Aggregation Characteristics for Bonding by Homophily

As adaptation principles are specified by the network characteristics of their reification, in particular the combination functions of the reification states for the adaptive connection weights, the properties of the aggregation are described as properties of such homophily combination functions. The following are considered plausible assumptions for a homophily combination function $\mathbf{c}(V_1, V_2, W)$ for reification state $\mathbf{W}_{X,Y}$ for $\omega_{X,Y}$; here $D = |V_1 - V_2|$:

- $\mathbf{c}(V_1, V_2, W)$ is a function: $[0, 1] \times [0, 1] \times [0, 1] \rightarrow [0, 1]$
- $\mathbf{c}(V_1, V_2, W)$ is a monotonically decreasing function of D
- For D close to 0 and $W < 1$ it holds $\mathbf{c}(V_1, V_2, W) > W$ (i.e., $\mathbf{W}_{\omega_{X,Y}}$ will increase)
- For D close to 1 and $W > 0$ it holds $\mathbf{c}(V_1, V_2, W) < W$ (i.e., $\mathbf{W}_{\omega_{X,Y}}$ will decrease)

Note that when the first condition is not fulfilled, usually the function is cut off at 1 (when its value would be above 1) or at 0 (when its value would be below 0); see also in Fig. 13.5. Relatively simple functions $\mathbf{c}(V_1, V_2, W)$ that satisfy these requirements are obtained when a *tipping point* τ (a fixed number between 0 and 1) is assumed such that for $0 < \mathbf{W}_{X,Y} < 1$ it holds

- upward change of $\mathbf{W}_{X,Y}$ when $D < \tau$ $\mathbf{c}(V_1, V_2, W) > W$ when $D < \tau$
- no change of $\mathbf{W}_{X,Y}$ when $D = \tau$ $\mathbf{c}(V_1, V_2, W) = W$ when $D = \tau$
- downward change of $\mathbf{W}_{X,Y}$ when $D > \tau$ $\mathbf{c}(V_1, V_2, W) < W$ when $D > \tau$

These criteria are formalised in the following definition of properties of any function $\mathbf{c}(V_1, V_2, W)$, but considered here as properties for homophily combination function in particular. So for the function $\mathbf{c}(V_1, V_2, W)$, keep in mind that this is

applied to a homophily combination function for reification state $\mathbf{W}_{X,Y}$ of $\mathbf{w}_{X,Y}$. It will be shown in Sect. 13.6 how these properties relate to the equilibrium behaviour of the network.

Definition 1 (Tipping point and strict tipping point)

- (a) The function $c(V_1, V_2, W): [0, 1] \times [0, 1] \times [0, 1] \rightarrow [0, 1]$ has *tipping point* τ for V_1 and V_2 if for all W with $0 < W < 1$ and all V_1, V_2 it holds
- (i) $c(V_1, V_2, W) > W \Leftrightarrow |V_1 - V_2| < \tau$
 - (ii) $c(V_1, V_2, W) = W \Leftrightarrow |V_1 - V_2| = \tau$
 - (iii) $c(V_1, V_2, W) < W \Leftrightarrow |V_1 - V_2| > \tau$
- (b) The function $c(V_1, V_2, W)$ has a *strict tipping point* τ if it has tipping point τ and in addition it holds:
- (i) If $|V_1 - V_2| < \tau$ then $c(V_1, V_2, 0) > 0$
 - (ii) If $|V_1 - V_2| > \tau$ then $c(V_1, V_2, 1) < 1$

Note Definition 1(a) can be reformulated in the sense that any function $c(V_1, V_2, W)$ that is monotonically decreasing in $D = |V_1 - V_2|$ and goes for any W with $0 < W < 1$ through the point with $D = |V_1 - V_2| = \tau$ and $c(V_1, V_2, W) = W$ has tipping point τ . This is illustrated in Fig. 13.5 by the yellow areas. In particular, this applies to all example functions shown in Table 13.2 as Fig. 13.5 shows that they all are monotonically decreasing and go through the point $(0.2, 0.7)$ for which $D = 0.2$ and $c(V_1, V_2, W) = 0.7$.

Note that condition (b) of this Definition 1 is not fulfilled when $|V_1 - V_2| < \tau$ and $c(V_1, V_2, 0) = 0$ or when $|V_1 - V_2| > \tau$ and $c(V_1, V_2, 1) = 1$. For example, for **slhomo** $_{\tau,\alpha}(V_1, V_2, W)$ and **sqhomo** $_{\tau,\alpha}(V_1, V_2, W)$ these cases do occur as always **slhomo** $_{\tau,\alpha}(V_1, V_2, 0) = 0$ and **slhomo** $_{\tau,\alpha}(V_1, V_2, 1) = 1$ due to the factor $W(1 - W)$, and the same for **sqhomo** $_{\tau,\alpha}(V_1, V_2, W)$. Therefore they do have a tipping point but they do not have a strict tipping point. In the third paragraph in Sect. 13.8 it is discussed how in a practical application having a tipping point but not having a strict tipping point is not a big problem, but some care is needed in not assigning initial values 0 or 1 to connection weights, as these values will never change in such cases. Note that when a function with strict tipping point τ is used, any two nodes X, Y with $\mathbf{w}_{X,Y}(t) = 0$ (which usually is interpreted as not being connected) can become connected over time: when $|X(t) - Y(t)| < \tau$, then by Definition 1(b)(i) it holds $\mathbf{W}_{X,Y}(t') > 0$ for $t' > t$.

Some examples of combination functions having a strict tipping point τ have been explored in more detail in Sharpanskykh and Treur (2014) and Boomgaard et al. (2018). In the former the advanced quadratic combination function **aqhomo** $_{\tau,\alpha}(V_1, V_2, W)$ and in the latter the advanced logistic function **alog2homo** $_{\tau,\sigma,\alpha}(V_1, V_2, W)$ has been explored; see also Treur (2016, Chap. 11, p. 309):

$$\begin{aligned}
\mathbf{aqhomo}_{\tau,\sigma}(V_1, V_2, W) &= W + \text{Pos}\left(\alpha\left(\tau^2 - (V_1 - V_2)^2\right)\right)(1 - W) \\
&\quad - \text{Pos}(-\alpha(\tau^2 - (V_1 - V_2)^2))W \\
\mathbf{alog2homo}_{\tau,\sigma,\alpha}(V_1, V_2, W) &= W + \text{Pos}\left(\alpha\left(0.5 - \frac{1 - W}{1 + e^{-\sigma(|V_1 - V_2| - \tau)}}\right)\right) \\
&\quad - \text{Pos}\left(-\alpha\left(0.5 - \frac{W}{1 + e^{-\sigma(|V_1 - V_2| - \tau)}}\right)\right)
\end{aligned} \tag{13.12}$$

Here $\text{Pos}(x) = (|x| + x)/2$. The following lemma shows some properties of this operator.

Lemma 1

- (a) $\text{Pos}(x) = x$ when x is positive, else $\text{Pos}(x) = 0$.
So always $\text{Pos}(x) \geq 0$, and when $\text{Pos}(x) > 0$, then $\text{Pos}(-x) = 0$.
- (b) For any numbers α and β the following are equivalent:
 - (i) $\alpha \text{Pos}(x) + \beta \text{Pos}(-x) = 0$
 - (ii) $\alpha \text{Pos}(x) = 0$ and $\beta \text{Pos}(-x) = 0$
 - (iii) $x = 0$ or $x > 0$ and $\alpha = 0$ or $x < 0$ and $\beta = 0$.

This format using the double $\text{Pos}(\cdot)$ function can often be used to create a combination function satisfying the strict tipping point condition as a variation on a combination function satisfying only the tipping point condition. This is shown in the following proposition that assumes any close distance function denoted by $d(\tau, D)$. More specifically, the following proposition makes it quite easy to obtain functions with tipping point τ or with strict tipping point τ . For a proof of these Propositions, see Chap. 15, Sect. 15.8.

Proposition 1 Suppose for any function $d(\tau, D)$ it holds

$$\begin{aligned}
d(\tau, D) &> 0 \quad \text{iff } D < \tau \\
d(\tau, D) &< 0 \quad \text{iff } D > \tau
\end{aligned}$$

Then the following hold:

- (a) For any $\alpha > 0$ the function

$$c(V_1, V_2, W) = W + \alpha W(1 - W) d(\tau, |V_1 - V_2|)$$

satisfies the tipping point condition, but not strict

(b) For any $\alpha > 0$ the function

$$c'(V_1, V_2, W) = W + \alpha \text{Pos}(d(\tau, |V_1 - V_2|))(1 - W) - \alpha \text{Pos}(-d(\tau, |V_1 - V_2|))W$$

satisfies the strict tipping point condition.

Proposition 1 can easily be applied to simple linear or quadratic functions $d(\tau, D)$ such as:

$$d(\tau, D) = \tau - D$$

$$d(\tau, D) = \tau^2 - D^2$$

but also to functions such as

$$d(\tau, D) = 0.5 - \frac{1}{1 + e^{-\sigma(D-\tau)}}$$

as is shown in Proposition 2(b) and (c).

The following proposition shows for four cases how it can be proven that some homophily combination function satisfies the tipping point or strict tipping point conditions. For proofs, see Chap. 15, Sect. 15.8.

Proposition 2

- (a) **log1hom** $_{\tau, \alpha}(V_1, V_2, W)$ has tipping point τ , and is not strict
- (b) **slog2hom** $_{\tau, \alpha}(V_1, V_2, W)$ has tipping point τ , and is not strict
- (c) **alog2hom** $_{\tau, \alpha}(V_1, V_2, W)$ has a strict tipping point τ
- (d) **exphomo** $_{\tau, \sigma}(V_1, V_2, W)$ has a tipping point τ and is not strict

The following proposition shows that weighted averages of functions with tipping point τ also have a tipping point τ , and the same for having a strict tipping point.

Proposition 3 A weighted average (with positive weights) of homophily combination functions with tipping point τ also has tipping point τ , and with strict tipping point τ , also has strict tipping point τ .

13.5.2 Relevant Aggregation Characteristics for Social Contagion

When more characteristics on network structure and adaptation combination functions are assumed, more refined results can be found, as will be shown in Sect. 13.6. Next, consider the combination functions used for social contagion of the states.

Definition 2 (Properties of combination functions for social contagion)

(a) A function $c(..)$ is called *monotonically increasing* if

$$U_i \leq V_i \text{ for all } i \Rightarrow c(U_1, \dots, U_k) \leq c(V_1, \dots, V_k)$$

(b) A function $c(..)$ is called *strictly monotonically increasing* if

$$U_i \leq V_i \text{ for all } i, \text{ and } U_j < V_j \text{ for at least one } j \Rightarrow c(U_1, \dots, U_k) < c(V_1, \dots, V_k)$$

(c) A function $c(..)$ is called *scalar-free* if $c(\alpha V_1, \dots, \alpha V_k) = \alpha c(V_1, \dots, V_k)$ for all $\alpha > 0$

Definition 3 (Normalised network) A network is *normalised* or uses normalised combination functions if for each state Y it holds $c_Y(\omega_{X_1,Y}, \dots, \omega_{X_k,Y}) = 1$, where X_1, \dots, X_k are the states from which Y gets incoming connections.

Note that $c_Y(\omega_{X_1,Y}, \dots, \omega_{X_k,Y})$ is an expression in terms of the parameter(s) of the combination function and $\omega_{X_1,Y}, \dots, \omega_{X_k,Y}$. To require this expression to be equal to 1 provides a constraint on these parameters: an equation relating the parameter value(s) of the combination functions to the parameters $\omega_{X_1,Y}, \dots, \omega_{X_k,Y}$. To satisfy this property, often the parameter(s) can be given suitable values. For example, for a Euclidean combination function $\lambda_Y = \omega_{X_1,Y}^n + \dots + \omega_{X_k,Y}^n$ will provide a normalised network. This can be done in general:

(1) normalisation by adjusting the combination functions. If any combination function $c_Y(..)$ is replaced by $c'_Y(..)$ defined as

$$c'_Y(V_1, \dots, V_k) = c_Y(V_1, \dots, V_k) / c_Y(\omega_{X_1,Y}, \dots, \omega_{X_k,Y})$$

then the network becomes normalised: indeed $c'_A(\omega_{X_1,Y}, \dots, \omega_{X_k,Y}) = 1$

(2) normalisation by adjusting the connection weights (for scalar-free combination functions). For scalar-free combination functions also normalisation is possible by adapting the connection weights; define:

$$\omega'_{X_i,Y} = \omega_{X_i,Y} / c_Y(\omega_{X_1,Y}, \dots, \omega_{X_k,Y})$$

Then the network becomes normalised; indeed it holds:

$$c_Y(\omega'_{X_1,Y}, \dots, \omega'_{X_k,Y}) = c(\omega_{X_1,Y} / c_Y(\omega_{X_1,Y}, \dots, \omega_{X_k,Y}), \dots, \omega_{X_k,Y} / c_Y(\omega_{X_1,Y}, \dots, \omega_{X_k,Y})) = 1$$

Definition 4 (Symmetric network and symmetric combination function)

a) A network is called *weakly symmetric* if for all states X, Y it holds $\omega_{X,Y} > 0 \Leftrightarrow \omega_{Y,X} > 0$. It is *fully symmetric* if for all states X, Y it holds $\omega_{X,Y} = \omega_{Y,X}$.

- b) A homophily combination function $c(V_1, V_2, W)$ is called *symmetric* if $c(V_1, V_2, W) = c(V_2, V_1, W)$.

If the homophily combination function $c(V_1, V_2, W)$ is symmetric, the network is fully symmetric if the initial values for $\omega_{X,Y}$ and $\omega_{Y,X}$ are equal. For a proof of the following proposition, again see Chap. 15, Sect. 15.8.

Proposition 4

- (a) When the homophily combination function $c(V_1, V_2, W)$ is symmetric, and initially the network is fully symmetric, then the network is continually fully symmetric.
- (b) For every $n > 0$ a Euclidean combination function of n th degree is strictly monotonically increasing, scalar-free, and symmetric.

13.6 Relating Adaptive Network Structure to Emerging Bonding Behaviour

In this section, an analysis is presented of the behaviour of an adaptive network based on the coevolution of social contagion and bonding by homophily. Here it is found out how the network and adaptation characteristics defined in Sect. 13.5 (such as a tipping point τ), affect the emerging behaviour of the adaptive network. This relates to horizontal arrow in the upper part of Fig. 13.1. In particular, it is addressed how these properties imply that over time the network ends up in certain states (for both the nodes and the connections) that represent community formation. It will turn out that under certain conditions in terms of the properties defined in Sect. 13.5, in the end, a number of communities emerge such that:

- Nodes within one community have similar state values
- Connections between nodes within a community are very strong
- Connections between nodes from different communities are very weak

Note that these phenomena were already observed in the simulation examples in Sect. 13.4, but now it will be proved why under certain conditions they always have to occur. To formalise this, the following general notions are important; e.g., Brauer and Nohel (1969), Hirsch (1984), Lotka (1956).

Definition 5 (Stationary point and equilibrium) A state Y has a *stationary point* at t if $\mathbf{d}Y(t)/\mathbf{d}t = 0$, is increasing at t if $\mathbf{d}Y(t)/\mathbf{d}t > 0$, and is decreasing at t if $\mathbf{d}Y(t)/\mathbf{d}t < 0$, and similarly this applies to reification states for adaptive connection weights ω . The network is in *equilibrium* at t if every state Y and every connection weight ω in the model has a stationary point at t . The equilibrium is *attracting* if any small perturbations of its values lead to convergence to the equilibrium values.

Considering the specific differential equation format for a temporal-causal network model shown in Sect. 13.2, and assuming nonzero speed factors the following more specific criteria for stationary points, and for increasing and decreasing trends, in terms of the combination functions and connection weights are easily found:

Lemma 2 (Criteria for a stationary, increasing and decreasing) Let Y be a state and X_1, \dots, X_k the states from which state Y gets its incoming connections. Then

- (i) Y has a stationary point at $t \Leftrightarrow \mathbf{c}_Y(\omega_{X_1,Y}X_1(t), \dots, \omega_{X_k,Y}X_k(t)) = Y(t)$
- (ii) Y is strictly increasing at $t \Leftrightarrow \mathbf{c}_Y(\omega_{X_1,Y}X_1(t), \dots, \omega_{X_k,Y}X_k(t)) > Y(t)$
- (iii) Y is strictly decreasing at $t \Leftrightarrow \mathbf{c}_Y(\omega_{X_1,Y}X_1(t), \dots, \omega_{X_k,Y}X_k(t)) < Y(t)$

Similarly this applies to reification states \mathbf{W} representing connection weights ω .

13.6.1 Relating Structure and Behaviour Independent of Social Contagion Characteristics

Theorem 1 presents some of the results found for the relation between the emerging equilibrium values for states and for connection weights. It is shown how the distance of the equilibrium values of two states relates to the equilibrium value of their connections. Note that for now no specific assumption is made on the aggregation characteristics for social contagion in terms of properties of the combination functions for it. To prove Theorem 1, the following lemma is a useful means. It shows that when the homophily combination function $c(V_1, V_2, W)$ satisfies the tipping point criterion, a connection weight 0 can only be reached for states X and Y when $|X(t) - Y(t)| > \tau$ and a connection weight 1 can only be reached for states X and Y when $|X(t) - Y(t)| < \tau$. For proofs, again see Chap. 15, Sect. 15.8.

Lemma 3 Suppose the function $c(V_1, V_2, W)$ has tipping point τ for V_1 and V_2 . Then

- (i) The value 0 for $\mathbf{W}_{X,Y}$ can only be reached from $\mathbf{W}_{X,Y}(t)$ with $0 < \mathbf{W}_{X,Y}(t) < 1$ if $|X(t) - Y(t)| > \tau$
- (ii) The value 1 for $\mathbf{W}_{X,Y}$ can only be reached from $\mathbf{W}_{X,Y}(t)$ with $0 < \mathbf{W}_{X,Y}(t) < 1$ if $|X(t) - Y(t)| < \tau$.

This lemma already reveals that connection weights $\omega_{X,Y}$ converging to 0 have some relation to the state values of X and Y having distance more than τ , and connection weights $\omega_{X,Y}$ converging to 1 have some relation to the state values of X and Y having a distance less than τ . These relations between connection weights and state values during a convergence process are made more precise for reaching an equilibrium state in Theorem 1.

Theorem 1 (Relations between equilibrium values for states and for connection weights) Suppose the function $c(V_1, V_2, W)$ has tipping point τ for V_1 and V_2

and an attracting equilibrium state is given with values \underline{X} for the states X and $\underline{W}_{X,Y}$ for the connection weight reification states $\underline{W}_{X,Y}$. Then the following hold:

- (a) If $|\underline{X} - \underline{Y}| < \tau$, then the equilibrium value $\underline{W}_{X,Y}$ is 1; in particular this holds when $\underline{X} = \underline{Y}$. Therefore, if $\underline{W}_{X,Y} < 1$, then $|\underline{X} - \underline{Y}| \geq \tau$, and, in particular, $\underline{X} \neq \underline{Y}$.
- (b) If $|\underline{X} - \underline{Y}| > \tau$, then the equilibrium value $\underline{W}_{X,Y}$ is 0. Therefore, if $\underline{W}_{X,Y} > 0$, then $|\underline{X} - \underline{Y}| \leq \tau$.
- (c) $0 < \underline{W}_{X,Y} < 1$ implies $|\underline{X} - \underline{Y}| = \tau$.

This Theorem 1 explains some of the observations made in Sect. 13.4, in particular, that in all of these simulations the connection weights all end up either in value 0 (the state equilibrium values differ at least τ) or in value 1 (the state equilibrium values are equal).

When also some assumptions are made for social contagion, more refined results can be found, for example, as explored in Treur (2018a). The following is a basic Lemma for normalised networks with social contagion combination functions that are monotonically increasing and scalar-free.

Lemma 4 Let a normalised network with nonnegative connections be given with combination functions that are monotonically increasing and scalar-free; then the following hold:

- (a)
 - (i) If for some state Y at time t for all nodes X with $\omega_{X,Y} > 0$ it holds $X(t) \leq Y(t)$, then $Y(t)$ is decreasing at t : $dY(t)/dt \leq 0$.
 - (ii) If, moreover, the combination function is strictly increasing and a state X exists with $X(t) < Y(t)$ and $\omega_{X,Y} > 0$, then $Y(t)$ is strictly decreasing at t : $dY(t)/dt < 0$.
- (b)
 - (i) If for some state Y at time t for all nodes X with $\omega_{X,Y} > 0$ it holds $X(t) \geq Y(t)$, then $Y(t)$ is increasing at t : $dY(t)/dt \geq 0$.
 - (ii) If, moreover, the combination function is strictly increasing and a state X exists with $X(t) > Y(t)$ and $\omega_{X,Y} > 0$, then $Y(t)$ is strictly increasing at t : $dY(t)/dt > 0$.

13.6.2 Relating Structure and Behaviour for Some Social Contagion Characteristics

Now the more specific theorem is obtained for the connection weights if the combination functions used for aggregation within social contagion for the states are assumed strictly monotonically increasing and scalar-free. It states that the

connection weights in an attracting equilibrium are all 0 or 1, and when τ is a strict tipping point, that depends just on whether they connect states with the same or a different equilibrium state value.

Theorem 2 (Equilibrium values $\underline{\mathbf{W}}_{X,Y}$ all 0 or 1) Suppose the network is weakly symmetric and normalised, and the combination functions for the social contagion for the base states are strictly monotonically increasing and scalar-free. Suppose that the combination functions $c(V_1, V_2, W)$ for the reification states for the connection weights have a tipping point τ . Then

- (a) In an attracting equilibrium state for any states X, Y from $\underline{\mathbf{X}} \neq \underline{\mathbf{Y}}$ it follows $\underline{\mathbf{W}}_{X,Y} = 0$.
- (b) In an attracting equilibrium state for any states X, Y with $\underline{\mathbf{X}} = \underline{\mathbf{Y}}$ it holds $\underline{\mathbf{W}}_{X,Y} = 0$ or $\underline{\mathbf{W}}_{X,Y} = 1$.
- (c) If $c(V_1, V_2, W)$ has a strict tipping point τ , then in an equilibrium state for any X, Y with $\underline{\mathbf{X}} = \underline{\mathbf{Y}}$ it holds $\underline{\mathbf{W}}_{X,Y} = 1$.

For proofs, see Chap. 15, Sect. 15.8. The following theorem shows the implications for emerging communities or clusters and distances between different equilibrium values for nodes.

Theorem 3 (Partition and equilibrium values of nodes) Suppose the network is weakly symmetric and normalised, the combination functions for the social contagion for the base states are strictly monotonically increasing and scalar-free, and the combination functions for the reification states for the connection weights use tipping point τ and is strict and symmetric. Then in any attracting equilibrium state a partition of the set of states into disjoint subsets C_1, \dots, C_p occurs such that:

- (i) For each C_i the equilibrium values for all the states in C_i are equal: $\underline{\mathbf{X}} = \underline{\mathbf{Y}}$ for all $X, Y \in C_i$.
- (ii) Every C_i forms a fully connected network with weights 1: $\underline{\mathbf{W}}_{X,Y} = 1$ for all $X, Y \in C_i$.
- (iii) Every two nodes in different C_i have connection weight 0: when $i \neq j$, then $X \in C_i$ and $Y \in C_j$ implies $\underline{\mathbf{W}}_{X,Y} = 0$.
- (iv) Any two distinct equilibrium values of states $\underline{\mathbf{X}} \neq \underline{\mathbf{Y}}$ have distance $\geq \tau$. Therefore there are at most $p \leq 1 + 1/\tau$ communities C_i and equilibrium values $\underline{\mathbf{X}}$.

13.7 Characterising Behaviour in Terms of Strongly Connected Components

To analyse connectivity, within Graph Theory the notion of a strongly connected component has been identified. The main parts of the following definitions can be found, for example, in Harary et al. (1965, Chap. 3), or Kuich (1970, Sect. 6). See also Chap. 12 of this volume.

Note that in the current chapter only nonnegative connection weights are considered.

Definition 6 (reachability and strongly connected components)

- (a) State Y is *reachable* from state X if there is a directed path from X to Y with nonzero connection weights and speed factors.
- (b) A network N is *strongly connected* if every two states are mutually reachable within N .
- (c) A state is called *independent* if it is not reachable from any other state.
- (d) A *subnetwork* of a network N is a network whose states and connections are states and connections of N .
- (e) A *strongly connected component* C of a network N is a strongly connected subnetwork of N such that it is maximal: no larger strongly connected subnetwork of N contains it as a subnetwork.

Strongly connected components C can be identified by choosing any node X of N and adding all nodes that are on any cycle through X . Note also that when a node X is not on any cycle, then it will form a singleton strongly connected component C by itself; this applies in particular to all nodes of N with indegree or outdegree zero. There are efficient algorithms available to determine the strongly connected components of a network or graph; for example, see Bloem et al. (2006), Fleischer et al. (2000), Gentilini et al. (2003), Łacki (2013), Li et al. (2014), Tarjan (1972), Wijs et al. (2016).

The strongly connected components form a partition of the nodes of the graph or network. By this partition a more abstract, simpler view of the network can be created, called condensation graph, in which each component becomes one abstract node; this is defined as follows.

Definition 7 (condensation graph) The *condensation graph* $C(N)$ of a network N with respect to its strongly connected components is a graph whose nodes are the strongly connected components of N and whose connections are determined as follows: there is a connection from node C_i to node C_j in $C(N)$ if and only if in N there is at least one connection from a node in the strongly connected component C_i to a node in the strongly connected component C_j .

An important result is that a condensation graph $C(N)$ is always an acyclic graph. In a sense, all cycles are locked up inside the components, and the connections between these components do not contain any cycles. The following theorem summarizes this; it was adopted from Harary et al. (1965, Chap. 3, Theorems 3.6 and 3.8), or Kuich (1970, Sect. 6).

Theorem 4 (Acyclic condensation graph)

- (a) For any network N its condensation graph $C(N)$ is acyclic, and has at least one state of outdegree zero and at least one state of indegree zero.
- (b) The network N is acyclic itself if and only if it is graph-isomorphic to $C(N)$. In this case, the nodes in $C(N)$ all are singleton sets $\{X\}$ containing one state X from N .
- (c) The network N is strongly connected itself if and only if $C(N)$ only has one node; this node is the set of all states of N .

Note that in an adaptive network, the strongly connected components and the condensation graph usually change over time. For example, connection weights that were 0 can become nonzero, or nonzero connection weights can converge to 0. From Theorem 3 it immediately follows that in the equilibrium state the C_i defined there are the strongly connected components of the network. Then the results from Theorem 3 can be rephrased in the above terms in the following way.

Theorem 5 (Strongly connected components in an attracting equilibrium)

Suppose the network is weakly symmetric and normalised, the combination functions for social contagion between the base nodes are strictly monotonically increasing and scalar-free, and the homophily combination functions for the connection weight reification states use tipping point τ and are strict and symmetric. Then in any attracting equilibrium state the following hold:

- (i) There are at most $p \leq 1 + 1/\tau$ strongly connected components.
- (ii) Each strongly connected component is fully connected and all states in it have a common equilibrium state value.
- (iii) There are no nonzero connections between states from different strongly connected components, and the equilibrium values of these states have distance $\geq \tau$.
- (iv) The condensation graph $C(N)$ is totally disconnected: it has no connections at all.

The following converse holds as well; this shows how equilibrium states can be characterised by specific properties of the strongly connected components. For a proof: Chap. 15, Sect. 15.8.

Theorem 6 (Strongly connected components characterisation)

Suppose the network is weakly symmetric, the combination functions for social contagion between the base nodes are strictly monotonically increasing, normalised and scalar-free, and the homophily combination function for the connection weight reification states use tipping point τ and are strict and symmetric. Suppose at some time point t the following hold:

- (i) Each strongly connected component C is fully connected and all states in C have a common state value.
- (ii) All connections between states from different strongly connected components have weight 0 and the equilibrium values of these states have distance $> \tau$.

Then the network is in an equilibrium state.

Note that the situation as characterised is a quite specific situation with trivial condensation graph, if compared, for example, to a general situation as addressed in Chap. 12 and Treur (2018c), where usually nontrivial condensation graphs occur.

13.8 Overview of Other Simulation Experiments

In recent years for a number of the functions from Table 13.2 simulation experiments have been performed for real-world domains and related to empirical data. An overview of them is shown in Table 13.4. Some of the experiences are the following.

In general, it was possible to get similar patterns as in the empirical data by using dedicated Parameter Tuning methods such as Simulated Annealing. As may be

Table 13.4 Overview of simulation experiments for different combination functions

Combination functions		Domain and data	Reference and venue
Homophily	Contagion		
slhomo _{σ,τ} (..)	ssum _{λ} (..)	Friendships in a classroom Glasgow data, 2016	Blankendaal et al. (2016) ECAI’16
		Social media: blogger appreciation Instagram data	Kozyreva et al. (2018) SocInfo’18
		Social media: music appreciation Twitter data	Gerwen et al. (2019) DCAI’18
	ssum _{λ} (..) alogistic _{σ,τ} (..)	Segregation of queer community Questionnaire data	Heijmans et al. (2019) ICICT’19
	alogistic _{σ,τ} (..)	Social media: Zwarte Piet debate Twitter data	Roller et al. (2017) COMPLEXNETWORKS’17
sqhomo _{σ,τ} (..)	ssum _{λ} (..)	Segregation of immigrants Literature data	Kappert et al. (2018) ICCCI’18
	alogistic _{σ,τ} (..)	Friendships in a classroom Glasgow data, 2016	Beukel et al. (2017, 2019) PAAMS’17, Neurocomputing 2019

(continued)

Table 13.4 (continued)

Combination functions		Domain and data	Reference and venue
Homophily	Contagion		
aqhomo _{σ, τ} (..)	ssum _{λ} (..)	Scalefree versus random networks Literature data	Sharpanskykh and Treur (2013, 2014) ICCCI'13, Neurocomputing 2014
log2homo _{σ, τ} (..)	ssum _{λ} (..)	Social media: physical activity Twitter data	Dijk and Treur (2018) ICCCI'18
	alogistic _{σ, τ} (..)	Friendships in a classroom Knecht data, 2008	Boomgaard et al. (2018) SocInfo'18

expected the remaining Root Mean Square error differed with the different studies and domains, and also depends on how fine-grained the scoring scales for the data were; for example when a 3 points scale was used for empirical data, already because of that in the $[0, 1]$ interval a variation of 0.15 should be expected within the empirical data themselves, and for a 5 points scale 0.1. Then an average deviation between model and empirical data will be at least in that order of magnitude, not smaller than, say 0.15–0.25. This indeed was usually the case in the examples discussed in Table 13.4.

Using the simple linear or simple quadratic functions **slhomo** _{σ, τ} (..) or **sqhomo** _{σ, τ} (..) the change of connection weights is very slow when the weights are close to 0 or 1 due to the factor $W(1 - W)$ in the function. The advantage of this slowing down effect is that the connection weight values stay within the $[0, 1]$ interval in a natural manner. But the downside of this factor is that when they are exactly 0 or 1 they will even freeze and not be able to change anyway, and the same when 0 or 1 are used as initial values. This is because **slhomo** _{σ, τ} (..) or **sqhomo** _{σ, τ} (..) have a tipping point, but no strict tipping point; also see the remark after Definition 1. The same holds for **log2homo** _{σ, τ} (..). So, when these functions are used, it is better to initialise all connection weight values between 0.1 and 0.9 instead of in the full $[0, 1]$ interval. This is different for the advanced linear and quadratic homophily functions **alhomo** _{σ, τ} (..) or **aqhomo** _{σ, τ} (..). For them approaching 0 or 1 is still slow, but leaving 0 or 1 can be fast: they do have a strict tipping point. Note, however, that this is not necessarily always a good property. Maybe when a very strong connection has been formed, even some differences that occur may not affect the connection immediately. So, in some cases, or for some types of persons the slow change close to 0 or 1 as shown by **slhomo** _{σ, τ} (..) or **sqhomo** _{σ, τ} (..) may even be more plausible.

Note that in Kozyreva et al. (2018) a slightly different multicriteria variant of the simple linear homophily function was used that takes into account multiple states in

the similarity measure: instead of $|V_1 - V_2|$ for 1 criterion, for k criteria the following Euclidean distance formula is used to measure similarity:

$$\sqrt{(V_{1,1} - V_{1,2})^2 + \dots + (V_{k,1} - V_{k,2})^2} \quad (13.13)$$

In Blankendaal et al. (2016) and Beukel et al. (2017) for bonding not only a homophily principle was used, but also a ‘more becomes more’ principle which can be considered a variant of what sometimes is called ‘the rich get richer’ (Simon 1955; Bornholdt and Ebel 2001), ‘cumulative advantage’ (de Solla Price 1976), ‘the Matthew effect’ (Merton 1968), or ‘preferential attachment’ (Barabási and Albert 1999; Newman 2003). For this ‘more becomes more’ principle, in Blankendaal et al. (2016) a scaled sum combination function was used for the (reified) weights of the connections to a given other person Y with scaling factor the number k of such connections (resulting in the average of these connection weights), and in Beukel et al. (2017, 2019) and advanced logistic sum:

$$\begin{aligned} \mathbf{ssum}_k(W_1, \dots, W_k) \\ \mathbf{alogistic}_{\sigma, \tau}(W_1, \dots, W_k) \end{aligned} \quad (13.14)$$

where W_1, \dots, W_k refer to the values of the reification states for the weights $\omega_{X_1, Y}, \dots, \omega_{X_k, Y}$ of all connections of the other person Y . Note that the first scaled sum option $\mathbf{ssum}_k(.)$ adapts to the other person’s average connection weight independent of the number of connections, whereas the second $\mathbf{alogistic}_{\sigma, \tau}(\dots)$ option is more additive as more connections of the other person provide higher values. In both approaches, the two combination functions for both the homophily and the more becomes more principle were combined as a weighted sum.

13.9 Discussion

In this chapter, it was analysed how emerging network behaviour (in particular, community formation) can be related to characteristics of the adaptive network’s structure for a reified adaptive network modeling bonding based on similarity. Parts of this chapter were adopted from Treur (2018b). Here the reified network structure characteristics include the aggregation characteristics in terms of the combination function specifying the adaptation principle incorporated. This has been addressed for adaptive social networks for bonding based on homophily (McPherson et al. 2001; Pearson et al. 2006) combined with social contagion for the base states. Relevant characteristics of the network and the adaptation principle have been identified, such as a tipping point for similarity for the combination function for the bonding. As one of the results, it has been found how the emergence of communities strongly depends on the value of this tipping point. It has been shown, for example, that some properties of the structure of the base network and the

adaptation principle modeled by the reification entail that the connection weights all converge to 0 (for persons in different communities) or 1 (for persons within one community). More specifically, it has been found how the formation of communities depends on the value τ of this tipping point: there can be no more communities than $1 + 1/\tau$, assuming state values within the interval $[0, 1]$.

The presented results do not concern results for just one type of network or combination function, as more often is found. Instead, they were formulated and proven at a more general level and therefore can be applied not just to specific networks but to classes of networks satisfying the identified relevant properties of network structure and adaptation characteristics. Note, however, that the focus in the current chapter is on deterministic behaviour; therefore stochastic models such as, for example, the one reported in a nontechnical manner in Axelrod (1997), are not covered by this analysis.

It may be an interesting research focus for the future to explore whether and how the analysis results found here have counterparts for stochastic network models. Besides, in Axelrod (1997) also regional differences are addressed. In a more extensive application of the models discussed in the current chapter, that may be an interesting ingredient to address as well.

The results found also have been related to the strongly connected components of the network (Harary et al. 1965, Chap. 3), or Kuich (1970, Sect. 6). A characterisation in terms of properties of the strongly connected components and their relations was found for states of an adaptive network which are attracting equilibrium states.

References

- Ashby, W.R.: Design for a Brain. Chapman and Hall, London (second extended edition) (1960) (First edition, 1952)
- Axelrod, R.: The dissemination of culture: a model with local convergence and global polarization. *J. Conflict Resolut.* **41**(2), 203–226 (1997)
- Barabási, A.L., Albert, R.: Emergence of scaling in random networks. *Science* **286**, 509–512 (1999)
- Blankendaal, R., Parinussa, S., Treur, J.: A temporal-causal modelling approach to integrated contagion and network change in social networks. In: Proceedings of the 22nd European Conference on Artificial Intelligence, ECAI'16. *Frontiers in Artificial Intelligence and Applications*, vol. 285, pp. 1388–1396. IOS Press (2016)
- Bloem, R., Gabow, H.N., Somenzi, F.: An algorithm for strongly connected component analysis in $n \log n$ symbolic steps. *Formal Method Syst. Des.* **28**, 37–56 (2006)
- Boomgaard, G., Lavitt, F., Treur, J.: Computational analysis of social contagion and homophily based on an adaptive social network model. In: Proceedings of the 10th International Conference on Social Informatics, SocInfo'18. *Lecture Notes in Computer Science*, vol. 11185, pp. 86–101. Springer Publishers (2018)
- Bornholdt, S., Ebel, H.: World Wide Webscaling exponent from Simon's 1955 model. *Phys. Rev. E* **64**, art. no. 035104 (2001)

- Brauer, F., Nohel, J.A.: *Qualitative Theory of Ordinary Differential Equations*. Benjamin (1969)
- de Solla Price, D.J.: A general theory of bibliometric and other cumulative advantage processes. *J. Am. Soc. Inform. Sci.* **27**, 292–306 (1976)
- Fleischer, L.K., Hendrickson, B., Pinar, A.: On identifying strongly connected components in parallel. In: Rolim, J. (ed.) *Parallel and Distributed Processing, IPDPS 2000. Lecture Notes in Computer Science*, vol. 1800, pp. 505–511. Springer (2000)
- Gentilini, R., Piazza, C., Policriti, A.: Computing strongly connected components in a linear number of symbolic steps. In: *Proceedings of the SODA'03*, pp. 573–582 (2003)
- Glasgow Empirical Data: https://www.stats.ox.ac.uk/~snijders/siena/Glasgow_data.htm (2016)
- Gross, T., Sayama, H. (eds.): *Adaptive Networks: Theory, Models and Applications*. Springer (2009)
- Harary, F., Norman, R.Z., Cartwright, D.: *Structural Models: An Introduction to the Theory of Directed Graphs*. Wiley, New York (1965)
- Heijmans, P., van Stijn, J., Treur, J.: Modeling cultural segregation of the queer community through an adaptive social network model. In: *Proceedings of the Fourth International Congress on Information and Communication Technology, ICICT'19. Advances in Intelligent Systems and Computing*. Springer (2019)
- Hirsch, M.W.: The dynamical systems approach to differential equations. *Bull. (New Ser.) Am. Math. Soc.* **11**, 1–64 (1984)
- Holme, P., Newman, M.E.J.: Nonequilibrium phase transition in the coevolution of networks and opinions. *Phys. Rev. E* **74**(5), 056108 (2006)
- Kappert, C., Rus, R., Treur, J.: On the emergence of segregation in society: network-oriented analysis of the effect of evolving friendships. In: Nguyen, N.T., Pimenidis, E., Khan, Z., Trawinski, B. (eds.) *Computational Collective Intelligence: 10th International Conference, ICCCI 2018, Proceedings*, vol. 1. *Lecture Notes in Artificial Intelligence*, vol. 11055, pp. 178–191. Springer (2018)
- Knecht, A.: Empirical data: collected by Andrea Knecht (2008). https://www.stats.ox.ac.uk/~snijders/siena/tutorial2010_data.htm
- Kozyreva, O., Pechina, A., Treur, J.: Network-oriented modeling of multi-criteria homophily and opinion dynamics in social media. In: Koltsova, O., Ignatov, D.I., Staab, S. (eds.) *Social Informatics: Proceedings of the 10th International Conference on Social Informatics, SocInfo'18*, vol. 1. *Lecture Notes in AI*, vol. 11185, pp. 322–335. Springer (2018)
- Kuich, W.: On the Entropy of Context-Free Languages. *Information and Control* **16**, 173–200 (1970)
- Kuipers, B.J.: Commonsense reasoning about causality: deriving behavior from structure. *Artif. Intell.* **24**, 169–203 (1984)
- Kuipers, B.J., Kassirer, J.P.: How to discover a knowledge representation for causal reasoning by studying an expert physician. In: *Proceedings of the Eighth International Joint Conference on Artificial Intelligence, IJCAI'83*. William Kaufman, Los Altos, CA (1983)
- Lacki, J.: Improved deterministic algorithms for decremental reachability and strongly connected components. *ACM Trans. Algorithms* **9**(3), Article 27 (2013)
- Levy, D.A., Nail, P.R.: Contagion: a theoretical and empirical review and reconceptualization. *Genet. Soc. Gen. Psychol. Monogr.* **119**(2), 233–284 (1993)
- Li, G., Zhu, Z., Cong, Z., Yang, F.: Efficient decomposition of strongly connected components on GPUs. *J. Syst. Architect.* **60**(1), 1–10 (2014)
- Lotka, A.J.: *Elements of Physical Biology*. Williams and Wilkins Co. (1924). Dover Publications, 2nd edn (1956)
- McPherson, M., Smith-Lovin, L., Cook, J.M.: Birds of a feather: homophily in social networks. *Ann. Rev. Sociol.* **27**(1), 415–444 (2001)
- Merton, R.K.: The Matthew effect in science. *Science* **159**(1968), 56–63 (1968)
- Newman, M.E.J.: The structure and function of complex networks. *SIAM Rev.* **45**, 167–256 (2003)

- Pearl, J.: Causality. Cambridge University Press (2000)
- Pearson, M., Steglich, C., Snijders, T.: Homophily and assimilation among sport-active adolescent substance users. *Connections* **27**(1), 47–63 (2006)
- Roller, R., Blommesteijn, S.Q., Treur, J.: An adaptive computational network model for multi-emotional social interaction. In: Proceedings of the 6th International Conference on Complex Networks and their Applications, COMPLEXNETWORKS'17. Studies in Computational Intelligence. Springer (2017)
- Sharpanskykh, A., Treur, J.: Modelling and analysis of social contagion processes with dynamic networks. In: Bădică, C., Nguyen, N.T., Brezovan, M. (eds.) Computational Collective Intelligence. Technologies and Applications. ICCCI 2013. Lecture Notes in Computer Science, vol. 8083, pp. 40–50. Springer, Berlin (2013)
- Sharpanskykh, A., Treur, J.: Modelling and analysis of social contagion in dynamic networks. *Neurocomputing* **146**(2014), 140–150 (2014)
- Simon, H.A.: On a class of skew distribution functions. *Biometrika* **42**(1955), 425–440 (1955)
- Tarjan, R.: Depth-first search and linear graph algorithms. *SIAM J. Comput.* **1**(2), 146–160 (1972)
- Treur, J.: Verification of temporal-causal network models by mathematical analysis. *Vietnam J. Comput. Sci.* **3**, 207–221 (2016a)
- Treur, J.: Network-Oriented Modeling: Addressing Complexity of Cognitive, Affective and Social Interactions. Springer Publishers (2016b)
- Treur, J.: Relating emerging network behaviour to network structure. In: Aiello, L.M., Cherifi, C., Cherifi, H., Lambiotte, R., Lió, P., Rocha, L.M. (eds.) Proceedings of the 7th International Conference on Complex Networks and their Applications, ComplexNetworks'18. Studies in Computational Intelligence, vol. 812, pp. 619–634. Springer Publishers (2018a)
- Treur, J.: Relating an adaptive social network's structure to its emerging behaviour based on homophily. In: Aiello, L.M., Cherifi, C., Cherifi, H., Lambiotte, R., Lió, P., Rocha, L.M. (eds.) Proceedings of the 7th International Conference on Complex Networks and their Applications, Complex Networks'18. Studies in Computational Intelligence, vol. 812, pp. 635–651. Springer Publishers (2018b)
- Treur, J.: Mathematical analysis of a network's asymptotic behaviour based on its strongly connected components. In: Proc. of the 7th International Conference on Complex Networks and their Applications, ComplexNetworks'18, vol. 1. Studies in Computational Intelligence, vol. 812, pp. 663–679. Springer Publishers (2018c)
- Treur, J.: Multilevel network reification: representing higher order adaptivity in a network. In: Proceedings of the 7th International Conference on Complex Networks and their Applications, ComplexNetworks'18, vol. 1. Studies in Computational Intelligence, vol. 812, pp. 635–651. Springer (2018d)
- Treur, J.: The ins and outs of network-oriented modeling: from biological networks and mental networks to social networks and beyond. *Trans. Comput. Collect. Intell.* **32**, 120–139 (2019). Text of Keynote Lecture at the 10th International Conference on Computational Collective Intelligence, ICCCI'18 (2018)
- Turnbull, L., Hütt, M.-T., Ioannides, A.A., Kininmonth, S., Poeppl, R., Tockner, K., Bracken, L.J., Keesstra, S., Liu, L., Masselink, R., Parsons, A.J.: Connectivity and complex systems: Learning from a multi-disciplinary perspective. *Appl. Netw. Sci.* **3**(47) (2018). <https://doi.org/10.1007/s41109-018-0067-2>
- van Beukel, S., Goos, S., Treur, J.: Understanding homophily and more-becomes-more through adaptive temporal-causal network models. In: De la Prieta, F. (ed.) Trends in Cyber-Physical Multi-Agent Systems. The PAAMS Collection—15th International Conference PAAMS'17. Advances in Intelligent Systems and Computing, vol. 619, pp. 16–29. Springer (2017)
- van Beukel, S., Goos, S., Treur, J.: An adaptive temporal-causal network model for social networks based on the homophily and more-becomes-more principle. *Neurocomputing* **338**, 361–371 (2019)

- van Dijk, M., Treur, J.: Physical activity contagion and homophily in an adaptive social network model. In: Nguyen, N.T., Pimenidis, E., Khan, Z., Trawinski, B. (eds.) *Computational Collective Intelligence: 10th International Conference, ICCCI 2018, Proceedings*. vol. 1. *Lecture Notes in AI*, vol. 11055, pp. 87–98. Springer (2018)
- van Gerwen, S., van Meurs, A., Treur, J.: An adaptive temporal-causal network for representing changing opinions on music releases. In: De La Prieta F., Omatu S., Fernández-Caballero, A. (eds.) *Distributed Computing and Artificial Intelligence, 15th International Conference, DCAI 2018. Advances in Intelligent Systems and Computing*, vol. 800, pp. 357–367. Springer, Cham (2019)
- Vazquez, F.: Opinion dynamics on coevolving networks. In: Mukherjee, A., Choudhury, M., Peruani, F., Ganguly, N., Mitra, B. (eds.) *Dynamics On and Of Complex Networks, Volume 2, Modeling and Simulation in Science, Engineering and Technology*, pp. 89–107. Springer, New York, (2013)
- Vazquez, F., Gonzalez-Avella, J.C., Eguíluz, V.M., San Miguel, M.: Time-scale competition leading to fragmentation and recombination transitions in the coevolution of network and states. *Phys. Rev. E* **76**, 046120 (2007)
- Wijs, A., Katoen, J.P., Bošnacki, D.: Efficient GPU algorithms for parallel decomposition of graphs into strongly connected and maximal end components. *Formal Methods Syst. Des.* **48**, 274–300 (2016)